Early Detection of Douglas-Fir Beetle Infestation with Subcanopy Resolution Hyperspectral Imagery

Rick Lawrence, *Department of Land Resources and Environmental Sciences, Montana State University, P.O. Box 173490, Bozeman, MT 59717; and* **Mari Labus,** *Research Systems, Inc., 4990 Pearl East Circle, Boulder, CO 80301.*

ABSTRACT: *Early detection of insect or pathogen infestations in forests would be useful to forest managers who want to make decisions that minimize timber losses. Typical methods of forest reconnaissance to detect infestations have included analysis of multispectral imagery. Multispectral imagery, however, often lacks the sensitivity to detect subtle changes in tree canopy reflectance because of physiologic stress from insects or pathogens. Most hyperspectral imaging has the sensitivity to detect subtle changes in canopy reflectance but lacks high spatial resolution to identify affected trees. Our study examined the use of subcanopy spatial resolution hyperspectral imagery for differentiating Douglas-fir trees attacked by the Douglas-fir beetle. Comparison of the accuracies of step-wise discriminant analysis and classification and regression tree analysis (CART) revealed that CART provided the best separability among tree health classes (93% overall) because of CART's ability to use different band combinations for each class. Predictive accuracy of the CART method was estimated through cross-validation of the dataset using a jackknife resampling technique. Overall classification accuracy was promising (69%), as was classification among healthy and attacked, but still living, trees (50–70%). The results of our study provide support that hyperspectral imagery might be used for detecting and mapping tree stress in Douglas-fir stands. Although the rapid progress of beetle infestation somewhat limited the ability to differentiate among tree stress classes, which might limit the utility of this approach for fast moving infestations, the results were well beyond what might be expected from alternative detection methods. Slower moving infestations would benefit from the use of hyperspectral imagery because a lower percentage of infested trees would be asymtomatic.*

Key Words: *Dendroctonus pseudotsugae, Pseudotsuga menziesii,* tree stress.

Early detection of forest diseases and insect infestations, such as beetle or root rot, is important to foresters who want to minimize economic loss due to these threats (Schmits and Gibson 1996). In rugged terrain where Douglas-fir (*Pseudotsuga menziesii*) often grows, this typically requires extensive field campaigns that are time-consuming and expensive. Remote sensing imagery from airborne and satellite-based sensors has been used in the past to map infestations but lacks the spectral sensitivity to detect infestations before visual signs of infestation become evident. Newer, hyperspectral instruments have this required sensitivity, providing information comparable to spectra obtained in the laboratory. These instruments, however, have lacked the

spatial resolution to map individual tree canopies. In the past several years, commercial high-resolution, hyperspectral imagery has become available with the introduction of Probe 1, operated by Earth Search Sciences, Inc., of McCall, ID, and HyMap, operated by HyVista Corporation of Sydney, Australia. Assessment of tree stress with the use of high-resolution, hyperspectral remote sensing might provide a method for detecting the early stages of infestation or disease over large areas more quickly and efficiently than by ground observations. Our objective was to determine if relative tree stress from Douglas-fir beetle (*Dendroctonus pseudotsugae*) could be detected using such imagery.

Insects, such as the Douglas-fir beetle, are considered agents of stress in forests because they adversely affect the physiology and growth of trees, often killing them. The Douglas-fir beetle occurs throughout much of the western United States, British Columbia, and Mexico (Schmitz and Gibson 1996, Thompson et al. 1996). These beetles normally attack and kill small groups of trees, but during outbreaks,

attacks on tree groups as large as 100 are not uncommon, especially in dense stands. Early evidence of infestation consists of entry holes in the tree bark and frass expelled from bark crevices by invading beetles. Several months after a successful infestation, foliage exhibits chlorosis by turning yellow, then sorrel, and then reddish brown, with needles beginning to fall from infested trees the year following attack.

As stresses occur, such as those from insect infestation, changes arise in leaf physiology, chemistry, and photosynthetic efficiency that affect the reflectance response of vegetation (Sampson et al. 1998). The detailed shape of the reflectance spectra and variables such as width, depth, skewness, and symmetry of absorption features can be measured and used to detect canopy stresses. For instance, leaf pigments, chlorophyll a&b, and chlorophyll fluorescence levels in leaves and needles of trees were highly related to visible and near infrared ratios and indices, particularly red edge indices, at the leaf and simulated canopy level (Sampson et al. 1998, Zarco-Tejada et al. 1999). Red edge indices are calculated along the red/infrared boundary, where chlorophyll absorption in vegetation forms one of the most extreme slopes found in spectra of naturally occurring materials. In healthy, green vegetation, the edge is sharp and steep, but as vegetation becomes stressed or senescence starts, the width of the absorption band decreases, and the red edge shifts towards shorter wavelengths (Clark et al. 1995). Red edge shifts have also been related to stress in crops that were sprayed with defoliant or water deprived (Clark et al. 1995). Other indices used to estimate physiologic responses in vegetation, such as the Physiological Reflectance Index (PRI), are calculated in the visible wavelengths. The PRI was highly correlated with xanthophyll pigments that are involved in part of the CO_2 assimilation process in vegetation and are a measure of photosynthetic efficiency. Substitution of other reflectance bands in the PRI calculation has resulted in better correlation with photosynthetic efficiency (CO_2 assimilated) in pine (Held and Jupp 1999). While these previous studies have shown that tree stress is detectable spectrally, most have been based on laboratory spectra. We sought to extend these studies to an operational level by using commercially available hyperspectral imagery to detect early stress caused by Douglas-fir beetle infestation at the individual tree or subcanopy level.

Methods

A Douglas-fir stand with known occurrence of Douglas-fir beetle infestation was located in the Lamar Valley of Yellowstone National Park, Wyoming. Sampled trees were selected randomly from 1:5000 scale color infrared aerial photos, were clustered into tree health classes based on field observations and were grouped as: (1) Healthy (H)—no sign of beetle infestation or other damage; (2) Attacked (A)—beetle infestation present as evidenced in bark, but the tree crown remains green with no visual signs of decline; and (3) Dead (D)—successful beetle infestation that has killed the tree within the past year, evidenced by red or yellow foliage. All trees sampled were dominant or subdominant and ranged from 0.5 to 2 m diameter at breast height.

A hyperspectral image swath of the sampled stand was collected at 10 a.m. on August 4, 1999 from the Probe-1 sensor. The sensor was flown aboard a helicopter at 500 m, producing $1 m^2$ pixel size with an approximately 0.5 km swath width. The sensor collected 128 continuous spectral bands in the visible through short-wave infrared (SWIR) spectral regions (0.4–2.5 μm). A 650 by 418 m study area subset of the image was analyzed. Georectification of the image was not performed due to unrecoverable image acquisition errors. Locational accuracy, however, was not required, since the high spatial resolution of the imagery made it possible to locate specific sample trees in the field and on the imagery. Spectral responses were extracted for image elements (pixels) for each sample tree (numbers of pixels per sampled tree ranged from 2 to 12, depending on how much of the sampled tree crown could be distinguished positively from other tree crowns). Total numbers of pixels for each of the tree health classes were 20 for healthy trees, 22 for attacked trees, and 13 for dead trees. Spectral responses were also extracted for other cover types within the study area, including light yellow (senescent) grass (LG) (18 pixels), heavy green grass (HG) (18 pixels), and shadow (SH) (18 pixels) to differentiate these spectral responses from the trees.

Individual and class average spectra were plotted for visual examination of among-class separability. We were able to apply analytical methods to the imagery that have been successfully developed for analyzing laboratory spectra because of the continuous spectral response provided by hyperspectral imagery. Although we examined several methods, the two best performing methods, stepwise discriminant analysis (DISCRIM) and classification and regression tree analysis (CART), were our primary statistical tools. In DISCRIM, predictor variables (spectral bands) are entered into the analysis based on their ability to increase group separation (tree health classes) (Huberty 1994). This reduces the number of spectral bands to a subset of bands that provides the best discrimination among classes. The subset of spectral bands is combined linearly into discriminant functions that describe the orthogonal (noncorrelated) dimensions in which classes reliably differ. The first discriminant function provides the best separation among classes, while the second function separates classes using information not used in the first function, and so on through all possible dimensions (Tabachnick and Fidell 1989). In this study, the first four discriminant functions were used to create four discriminant images and combined into one "multispectral" discriminant image. A supervised classification was then performed on the discriminant image.

CART analysis involves binary recursive partitioning to determine which single explanatory variable best reduces deviance in the response variable (Breiman et al. 1984, Friedl and Brodley 1997, Lawrence and Ripple 2000). Each possible binary split for all variables is evaluated recursively for best class separability until homogeneous end points are reached in a hierarchical tree. In this study, all sampled class spectra were introduced in CART as explanatory variables and used to develop the splitting rules for assigning classes. The tree was evaluated as to whether all terminal nodes significantly reduced

deviance and pruned back to a level believed to be not overfit. The splitting rules were used in a rule-based approach to create a classified image.

The classification methods were compared for overall accuracy, Kappa (which estimates classification accuracy compared to a random assignment), and individual class user's and producer's accuracies (user's accuracy measures errors of commission or the accuracy of resulting maps, while producer's accuracy measures errors of omission (Congalton and Green 1999). The method that produced the highest overall accuracy was subject to an intensive cross-validation procedure using a jackknife resample technique. In jackknife resampling, bias is reduced in small datasets by leaving each sample out and developing the classification from all other cases. The withheld sample is then classified, added back into the dataset, the next sample is taken out of the dataset, and the procedure is repeated until all samples have been evaluated.

Results

Examination of spectral responses from individual trees showed classes grouping at different reflectance values in specific wavelengths, such as in the two sharp peaks at 1,000 and 1,100 nm, the wider peak around 1,250 nm, and in the two large peaks at >1,500 nm (Figure 1 shows these spectral ranges for the class averages). There were also considerable overlaps among different classes in certain portions of the spectrum, even within those regions where some class separability existed. For example, only class SH separated well from the other classes in all portions of the spectrum due to the very low reflectance of shadow. In the visible wavelengths, no vegetation class showed substantial separability. At the near infrared (NIR)

boundary (700 to 750 nm) and in the short-wave IR region (especially 1,100 to 1,200 nm), where vegetation characteristics typically stand out, the D class was differentiated from the spectra of other green vegetation, but the H and A classes fail to differentiate. HG was separated from other classes with very high reflectance values within the 750–800 nm and 1,000–1,100 nm range, was strongly mixed with other spectra in the 1,500–1,750 nm range, and then again separated into its own group in the 2,000–2,500 nm, though with intermediate reflectance values at this wavelength. The H and D classes separated well in the 1,500–1,750 nm and 2,000–2,500 nm ranges, while the A class spectra overlapped the H class in these wavelengths.

Examination of average class spectra gave a clearer overview of class separability (Figure 1). Green vegetation separated from the D class in the peaks of the 700–800 nm and the 1,000–1,375 nm ranges. In the visible range, all classes except for shadow were confounded. Two sharp reflectance peaks at 1,007 and 1,069 nm showed promise for good class separability in all classes. At longer wavelengths (1,500–2,500nm), grasses (heavy and light) were confounded with the D class. It was also evident that the averaged A spectrum was very similar to the H class, indicating poor separability for this important class at these longer wavelengths.

DISCRIM used 17 spectral bands to distinguish the classes (Table 1). The first four discriminant functions accounted for approximately 95% of the variability in the classes. CART, on the other hand, used only six of the spectral bands (Figure 2) to account for 91% of the variability.
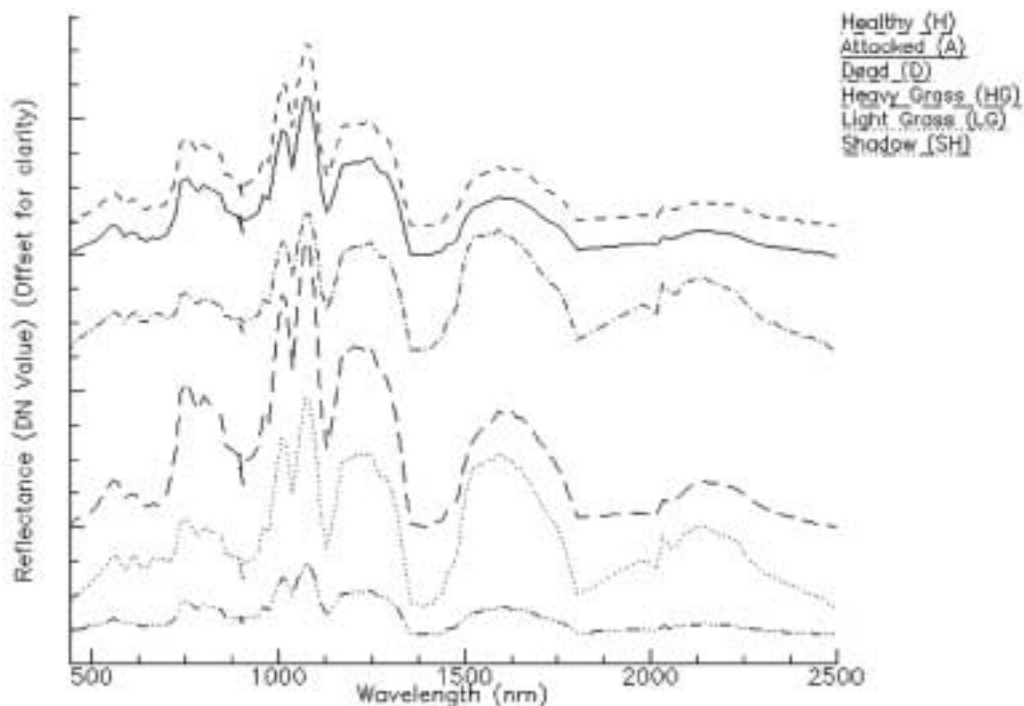
CART provided superior classification results compared

Figure 1. Class spectra averages showing class distinctions. Spectral responses are offset on the y-axis to improve visual differentiation of similar spectra.

Table 1. Spectral bands (central band wavelength in nm) and discriminant function weightings used in the DISCRIM classification.

Spectral band (nm)	Function			
	1	2	3	4
448.60	−1.107	−0.186	0.806	−1.029
509.10	−1.354	0.247	4.763	−2.207
523.80	−5.142	0.251	−6.791	0.629
539.90	−4.337	−2.210	4.630	1.690
600.60	12.886	0.943	−4.194	5.395
707.50	−0.700	3.019	1.866	−5.175
738.00	−2.678	−7.690	−1.130	0.586
767.80	2.289	16.081	1.901	−3.803
876.60	0.470	−9.724	−0.044	4.449
1422.60	0.913	0.353	−0.917	0.574
1466.40	0.003	−2.337	2.725	−5.963
1801.10	1.465	−0.495	−0.509	−0.692
2071.10	−1.235	3.125	−1.519	9.609
2089.50	4.895	7.299	6.818	−5.300
2282.60	−3.989	−7.867	−8.668	0.142
2382.10	−1.725	−1.846	−0.309	2.865
2430.40	0.029	1.171	2.065	−0.299

to DISCRIM (Table 2), as well as all other methods tested. CART had an overall accuracy of 92.5% and a Kappa of 0.91 and produced a 100% user's accuracy in the important A class and a 74% accuracy in the H class. Accuracy for the D class was 90%, while the LG and HG classes achieved 100% accuracy. The DISCRIM approach could not readily distinguish in the H and A classes. High accuracies were achieved by DISCRIM in the D, LG, and HG classes.

Overall accuracy for the CART method using the jackknife resampling technique was 69%, and the Kappa was 0.62. User's accuracy for the A class was 53%. Poor distinction between the A and H classes persisted, with user's accuracy for the H class at 57%. Poor distinction also was present between the D and LG classes, with user's accuracies of 59 and 75%, respectively. The HG class was well distinguished from other classes (100% user's accuracy), while the SH class was not well distinguished from the H class.
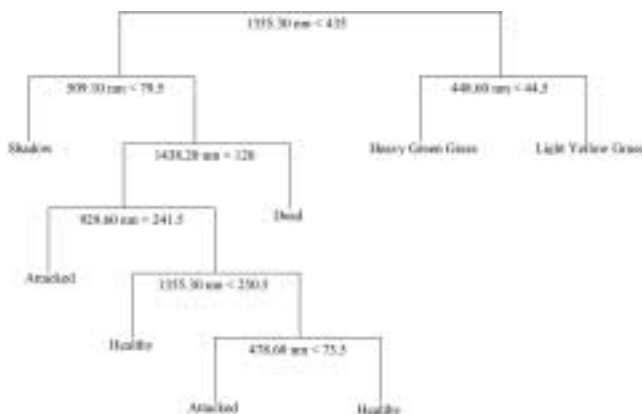

Figure 2. CART tree developed using all samples. The tree shows utilized spectral bands (designated by central band wavelength) and splitting rules for classification. Splitting rules apply to the left branchings of the tree.

Discussion

Our analysis demonstrated that subcanopy resolution hyperspectral imagery could successfully distinguish among tree stress classes resulting from Douglas-fir beetle attack. Examination of the classification methods showed that the CART approach provided the best ability to separate tree health classes. CART's ability to use different band combinations for each class in a rule-based classification allowed for maximum spectral separability of tree health classes compared to DISCRIM, which required the same spectral bands for all classes. This was advantageous because tree health classes and other background classes were different in their physical and chemical characteristics, and thus spectral regions in which classes could be distinguished varied. The mean spectral profiles for each class showed these class spectra and the spectral regions where class distinctions could be made. Although the spectra were similar, slight shifts in the spectral regions of maximum separation could be seen in all classes. CART utilized these slight differences in the spectra to build the classification tree, thus it took full advantage of spectral resolution afforded by hyperspectral imagery and reduced the spectral data to those bands that provided the best class distinctions.

Results of the classification using the CART-Jackknife method were encouraging for the use of hyperspectral imagery for mapping tree stress. Use of the jackknife method of cross-validation in combination with CART allowed for a realistic estimate of the ability of CART to separate groups while reducing bias associated with our dataset for validation. Some confusion persisted between H and A classes using CART-Jackknife, with the best class accuracies from 50 to 70%. This confusion was the result of substantial variability in spectral responses among trees within these tree health classes.

Tree response to beetle attack occurs over a relatively short time period compared to other, slow-acting stressors such as root rot. Time between initial attack and visual signs of chlorosis can be as short as a month, with death occurring

Table 2. Accuracies and kappa statistics for the classification methods.

Accuracy (%)	Classes	DISCRIM	CART	CART-Jack
Producers	H	32.5	100	70.0
	A	47.8	65.2	50.0
	D	89.5	100	84.2
	LG	97.2	100	50.0
	HG	100	100	88.9
	SH	100	100	80.6
Users	H	50.0	74.1	57.1
	A	51.7	100	53.5
	D	70.8	90.5	59.3
	LG	76.1	100	75.0
	HG	100	100	100
	SH	94.7	100	100
Overall		74.6	92.5	68.6
Kappa statistic		0.69	0.91	0.62

within 2–3 months (Thompson et al. 1996, Zarco-Tejada et al. 1999). This means that there will be large proportions of trees that have been recently attacked (i.e., exhibit evidence of boring) that are not yet experiencing stress, visual or otherwise. If the imagery is detecting nonvisible indicators of tree stress, this inclusion of not yet stressed trees might have limited our accuracy. For trees infested with more slowly advancing pathogens, such as root rot, the relatively slower advance of the disease means a smaller proportion of nondetectable recent infestations, reduced variability in the spectral response of the infested class, and an increased chance of identifying trees and outbreak areas. We would, therefore, expect superior results with slower advancing infestations. If a particular source of tree stress resulted in increased spectral variability, however, classification results might be lower.

Our study has shown that CART analysis of remote sensing data is a robust and easily implemented statistical method of classification without the need of extensive expert knowledge. This study was conducted in a single stand having one species and a single known source of tree stress, and further studies will be necessary to determine how broadly our results are applicable. At least in this case, however, CART effectively created classification rules that distinguished the early stages of tree stress by using the full spectral capabilities of hyperspectral imagery. Thus, the possibility exists that hyperspectral imagery of large forest stands might be useful in identifying areas of relative tree stress that would not otherwise be detected without prohibitive field reconnaissance. Forest stands classified as experiencing higher stress could then be examined on the ground to identify the causes of the stress (e.g., beetle attack, root rot, poor site conditions). Ameliorative actions, if available, can be taken at earlier stages, thus reducing adverse economic and forest health effects.

Literature Cited

BREIMAN, L., J.H. FRIEDMAN, R.A. OLSHEN, AND C.J. STONE. 1984. Classification and regression trees. Wadsworth International Group, Belmont, CA. 358 p.

CLARK, R.N., T.V.V. KING, C. AGER, AND G.A. SWAYZE. 1995. Initial vegetation species and senescence/stress indicator mapping in the San Luis Valley, Colorado using imaging spectrometer data. P. 64-69 in Proc. of Summitville Forum '95, Posey, H.H., J.A. Pendelton, and D. Van Zyl (eds.). Colorado Geolog. Surv. Spec. Publ. 38.

CONGALTON, R.G., AND K. GREEN. 1999. Assessing the accuracy of remotely sensed data: Principles and practices. Lewis Publishers, New York. 137 p.

FRIEDL, M.A., AND C.E. BRODLEY. 1997. Decision tree classification of land cover from remotely sensed data. Rem. Sens. Environ. 61:399–409.

HELD, A.A., AND D.L.B. JUPP. 1999. Forest monitoring with high spectral/spatial remote sensing tools: Case studies. CSIRO Div. of Water Resour., Canberra ACT. http://ltpwww.gsfc.nasa.gov/ISSSR-95/forestmo.htm

HUBERTY, C.J. 1994. Applied discriminant analysis. Wiley, New York. 466 p.

LAWRENCE, R.L., AND W.J. RIPPLE. 2000. Fifteen years of revegetation of Mount St. Helens: A landscape-scale analysis. Ecology 81:2742–2752.

SAMPSON, P.H., G.H. MOHAMMED, S.J. COLOMBO, T.L. NOLAND, J.R. MILLER, AND P.J. ZARCO-TEJADA. 1998. Bioindicators of forest sustainability. Progress Report. Ontario For. Res. Inst., Sault Ste. Marie, ON, For. Res. Info. Pap. No. 142.

SCHMITZ, R.F., AND K.E. GIBSON. 1996. Douglas-fir Beetle. USDA For. Serv. For. Insect & Dis. Leafl. 5. R1-96-87. Washington, D.C.

TABACHNICK, B.G., AND L.S. FIDELL. 1989. Using multivariate statistics. Ed. 2. Harper Collins Publishers, New York. 746 p.

THOMSON, A.J., D.G. GOODENOUGH, H.J. BARCLAY, Y.J. LEE, AND R.N. STURROCK. 1996. Effects of laminated root rot (Phellinus weirii) on Douglas-fir foliar chemistry. Can. J. For. Res. 26:1440–1445.

ZARCO-TEJADA, P.J., J.R. MILLER, G.H. MOHAMMED, T.L. NOLAND, AND P.H. SAMPSON. 1999. Canopy optical indices from infinite reflectance and canopy reflectance models for forest condition monitoring: Applications to hyperspectral CASI data. P. 1–4 in Proc. of the IEEE Internat. Geosci. and Rem. Sens. Symp. IGARSS, Hamburg, Germany.